

VI-I Photoionization and Photodissociation Dynamics Studied by Electron and Fluorescence Spectroscopy

Molecular photoionization is a major phenomenon in vacuum UV excitation and provides a large amount of information on fundamental electron-core interactions in molecules. Especially, neutral resonance states become of main interest, since they often dominate photoabsorption cross sections and lead to various vibronic states which are inaccessible in direct ionization. We have developed a versatile machine for photoelectron spectroscopy in order to elucidate dynamical aspects of superexcited states such as autoionization, resonance Auger decay, predissociation, vibronic couplings, and internal conversion. Two-dimensional photoelectron spectroscopy, allows us to investigate superexcited states in the valence excitation region of acetylene, nitric oxide, carbonyl sulfide, sulfur dioxide and so on. In this method, the photoelectron yield is measured as a function of both photon energy and electron kinetic energy (binding energy). The spectrum, usually represented as a contour plot, contains rich information on photoionization dynamics.

Photofragmentation into ionic and/or neutral species is also one of the most important phenomena in the vacuum UV excitation. In some cases, the fragments possess sufficient internal energy to de-excite radiatively by emitting UV or visible fluorescence. It is widely accepted that fluorescence spectroscopy is an important tool to determine the fragments and to clarify the mechanisms governing the dissociation processes of diatomic and polyatomic molecules. This year we have carried out fluorescence spectroscopy of H₂O in the photon energy region of 15–30 eV.

VI-I-1 Formation and Autoionization of a Dipole-Forbidden Superexcited State of CS₂

HIKOSAKA, Yasumasa¹; MITSUKE, Koichiro
(¹*Inst. Mater. Struct. Sci.*)

[*J. Phys. Chem. A* **105**, 8130 (2001)]

Two-dimensional photoelectron spectroscopy has been performed in the photon energy region of 14.60–15.35 eV, to investigate forbidden superexcited states of CS₂. The two-dimensional photoelectron spectra for the CS₂⁺($\tilde{X}^2\Pi_g$) and CS₂⁺($\tilde{B}^2\Sigma_u^+$) bands show remarkable formation of vibrational levels excited with one quantum of the antisymmetric stretch vibrational mode at $E_{hv} \sim 14.88$ eV. This vibrational excitation is attributable to autoionization from a dipole-forbidden superexcited state which is formed through vibronic interaction with the $5p\sigma_u$ Rydberg state converging to CS₂⁺($\tilde{C}^2\Sigma_g^+$). The forbidden superexcited state is assigned as the $v = 1$ vibrational state in the ν_3 mode of the $3d\sigma_g$ Rydberg member converging to CS₂⁺($\tilde{C}^2\Sigma_g^+$). Preference in the autoionization of the forbidden superexcited state was discussed.

VI-I-2 Autoionization and Neutral Dissociation of Superexcited HI Studied by Two-Dimensional Photoelectron Spectroscopy

HIKOSAKA, Yasumasa¹; MITSUKE, Koichiro
(¹*Inst. Mater. Struct. Sci.*)

Two-dimensional photoelectron spectroscopy of hydrogen iodide has been performed in the photon energy region of 11.10–14.85 eV, in order to investigate dynamical properties on autoionization and neutral dissociation of Rydberg states HI*(R_A) converging to HI⁺($\tilde{A}^2\Sigma^+_{1/2}$). A two-dimensional photoelectron spectrum in Figure 1 exhibits strong vibrational excitation of HI⁺($\tilde{X}^2\Pi_{3/2}$) over a photon energy region from ~ 12 to 13.7 eV, which is attributable to autoion-

izing feature of the $5d\pi$ HI*(R_A) state. Noticeable features around the photon energy region of 13.5–14.5 eV are assigned as resulting from autoionizing transitions from I* [converging to I⁺(3P_0 or 1)] into I⁺(3P_2). The formation mechanism of I* is due to the predissociation of HI*(R_A) by the repulsive HI* state of Rydberg type converging to HI⁺($^4\Pi_{1/2}$).

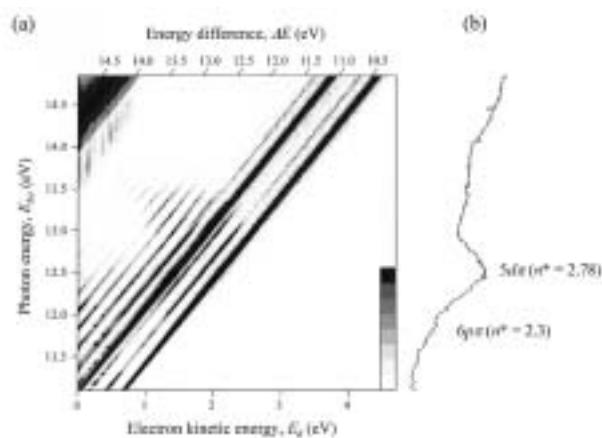


Figure 1. (a) Two-dimensional photoelectron spectrum of HI in the photon energy range of 11.10–14.85 eV. The electron yield, measured as a function of both photon energy E_{hv} and electron kinetic energy E_k , is presented by the plots with eight tones from light to dark on a linear scale. The intense structures are truncated. Diagonal lines attached on the top of this figure denote the energy difference defined by $\Delta E = E_{hv} - E_k$. (b) The curve obtained by summing electron counts over the whole range of E_k as a function of E_{hv} .

VI-I-3 Development of the Apparatus for High-Resolution Dispersed Spectroscopy and Fluorescence Excitation Spectroscopy at BL3A2

MITSUKE, Koichiro

The fluorescence was collected by an optical detec-

tion device in Figure 1 made up of spheroidal and spherical mirrors facing each other across the photoexcitation region (*PR*), *i.e.* the source of the fluorescence.¹⁾ One focal point of the spheroidal mirror fell at *PR*, while the other focal point was at the surface of an optical-fiber bundle. The fluorescence light was reflected back to *PR* by the spherical mirror and was then focused onto the surface of the fiber bundle by the spheroidal mirror. This detection system can collect light from about 62% of the full-sphere solid angle. The fluorescence passed through the optical-fiber bundle (transmission ~ 55% at 400 nm).

In dispersed fluorescence spectroscopy we utilized a 300 mm focal-length imaging spectrograph equipped with a liquid-nitrogen cooled CCD array detector. The overall detection efficiency, including the two mirrors, fiber bundle, and imaging spectrograph, was estimated to be $(1-5) \times 10^{-3}$ with the slit width of the spectrograph being 250 μm . When we fulfilled fluorescence excitation spectroscopy by scanning the wavelength of synchrotron radiation, we replaced the CCD array detector by a photomultiplier tube. In this case, the overall detection efficiency was estimated to be $(1.4 \pm 0.3) \times 10^{-3}$ at the slit widths of the monochromator of 2 mm. All spectra were corrected by the wavelength dependence of the relative detection efficiency.

Reference

- 1) K. Mitsuke and M. Mizutani, *Bull. Chem. Soc. Jpn.* **74**, 1193 (2001).

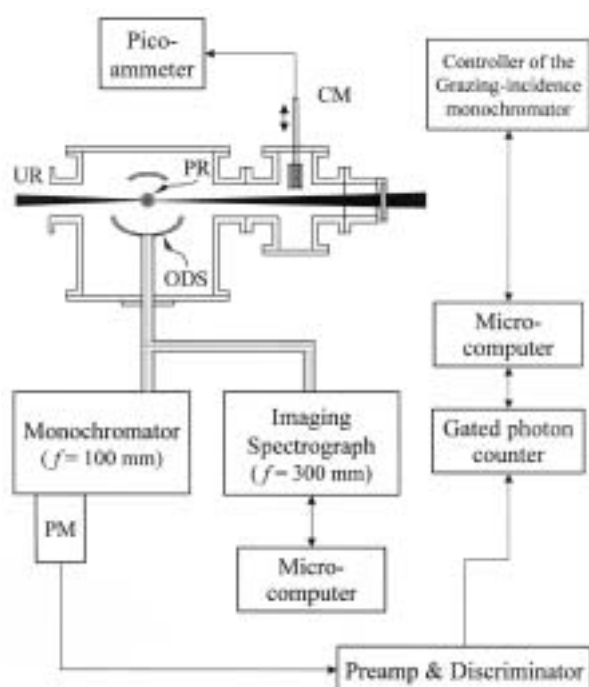


Figure 1. Schematic diagram of the apparatus for dispersed fluorescence spectroscopy and fluorescence excitation spectroscopy. UR, monochromatized undulator radiation; PR, photoexcitation region (not to scale); ODS, optical detection system composed of two mirrors and an optical-fiber bundle; CM, gold-mesh current monitor; PM, photomultiplier.

VI-I-4 UV and Visible Dispersed Spectroscopy for the Photofragments Produced from H₂O in the Extreme Ultraviolet

MITSUKE, Koichiro

[*J. Chem. Phys.* **117**, 8334 (2002)]

The photofragmentation of H₂O has been studied by fluorescence spectroscopy in the photon energy region between $E_{h\nu} = 16.9-54.5$ eV at the beam line 3A2 of UVSOR. The fluorescence in the wavelength range of 280–720 nm was dispersed with an imaging spectrograph. The dispersed spectra in Figure 1 exhibit the hydrogen Balmer lines of $\text{H}^*[n^2L', J' \rightarrow 2^2L'', J'']$ ($n = 3-9$) and the emission band systems of $\text{H}_2\text{O}^+ [\tilde{A}^2A_1(0, v', 2, 0) \rightarrow \tilde{X}^2B_1(0, 0, 0)]$, $[\text{OH}^+(\tilde{A}^3\Pi_Q, v' \rightarrow \tilde{X}^3\Sigma^-, v'')]$, and $[\text{OH}^+(\tilde{A}^2\Sigma^+, v' \rightarrow \tilde{X}^2\Pi_Q, v'')]$. The fluorescence cross sections for these transitions have characteristic dependences on $E_{h\nu}$ and vibrational quantum numbers. The cross section summed over the Balmer lines takes a minimum value at $E_{h\nu} = 21.7$ eV and is very small even at 24.9 eV beyond which it steadily increases with increasing $E_{h\nu}$. This behavior is understood as that the superexcited states correlating with $\text{H}^*(n \geq 3) + \text{OH}(\tilde{A}^2\Sigma^+)$ are too repulsive to be accessible below $E_{h\nu} \sim 30$ eV by the Franck-Condon transitions from $\text{H}_2\text{O}(\tilde{X}^1A_1)$ and as that the Balmer emission below 30 eV is mainly due to the $\text{H}^*(n \geq 3) + \text{H}(n = 1) + \text{O}(^3P_g)$ channel. The appearance energy 25.5 ± 0.3 eV of the $\text{OH}^+(\tilde{A}^3\Pi_Q, v' \rightarrow \tilde{X}^3\Sigma^-, v'')$ transitions is much higher than the dissociation limit of 21.5 eV for the $\text{OH}^+(\tilde{A}^3\Pi_Q) + \text{H}(n = 1)$ channel, but is consistent with the vertical ionization energy to $\text{H}_2\text{O}^+[(1b_1)^{-2}(4a_1)^1 2A_1]$ that has been assumed to correlate with the above dissociation limit. The vibrational distribution of $\text{OH}^+(\tilde{A}^3\Pi_Q)$ evaluated from the $\text{OH}^+(\tilde{A}^3\Pi_Q, v' \rightarrow \tilde{X}^3\Sigma^-, v'')$ band intensities is similar to the prior distribution in the rigid-rotor harmonic-oscillator approximation.

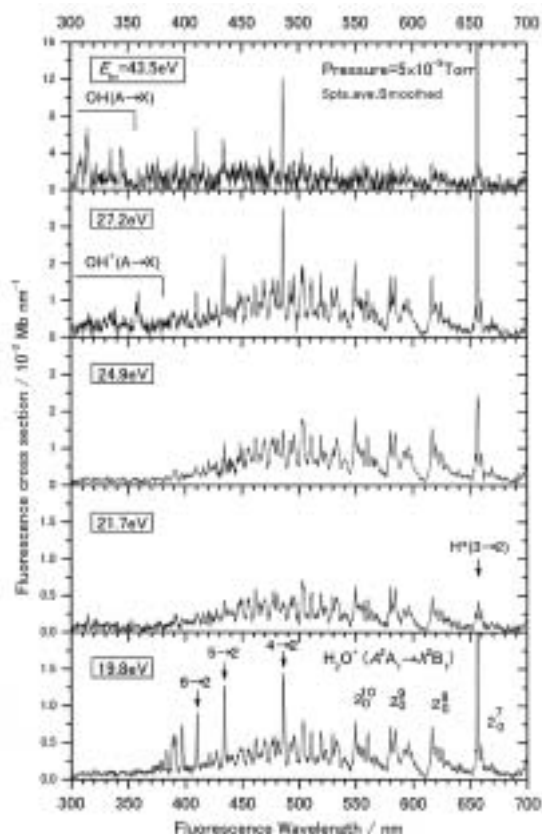


Figure 1. Dispersed fluorescence spectra of H₂O encompassing the wavelength region 300–700 nm at six photon energies between $E_{h\nu} = 19.8$ and 43.5 eV. The $2_0^{v_2}$ symbols in the panel of $E_{h\nu} = 21.7$ eV designate the vibrational progression in the bending mode v_2 of the H₂O⁺[$\tilde{A}^2A_1(0, v_2, 0) \rightarrow \tilde{X}^2B_1(0, 0, 0)$] transition. The hydrogen Balmer lines H* [$n^2L'J' \rightarrow 2^2L''J''$ ($n = 3-9$)] are indicated by the ($n \rightarrow 2$) marks.

VI-J Vacuum UV Spectroscopy Making Use of a Combination of Synchrotron Radiation and a Mode-Locked or Pulsed UV Laser

An ultraviolet laser system has been developed which synchronizes precisely with the synchrotron radiation (SR) from the storage ring of the UVSOR facility. A mode-locked Ti:sapphire laser is made to oscillate at the frequency of the ring in a multibunch operation mode. The delay timing between SR and laser pulses can be changed from 0 to 11 ns. The following combination studies have been performed: (1) two-photon ionization of helium atoms studied as the prototype of the time-resolved experiment, (2) laser induced fluorescence (LIF) excitation spectroscopy of N₂⁺($X^2\Sigma_g^+$) ions produced by synchrotron radiation photoionization of N₂ or N₂O, and (3) LIF excitation spectroscopy of CN($X^2\Sigma^+$) radicals produced by synchrotron radiation photodissociation of CH₃CN.

VI-J-1 Partial Photoionization Cross Sections for N₂⁺($X^2\Sigma_g^+$, $v_X = 0, 1$) Measured by a Laser Synchrotron Radiation Combination Technique

MITSUKE, Koichiro; MATSUMURA, Hisashi¹
(¹Chiba Univ.)

[*J. Electron Spectrosc. Relat. Phenom.* submitted]

Molecular superexcited states undergo autoionization into various vibrational levels of a low-lying ionic state with branching ratios BR considerably different from those for the direct ionization. The BR values are determined chiefly by the molecular constants on the potential energy surfaces involved and transition pro-

abilities for autoionization. In this study, N₂ is subjected to photoionization with the monochromatized undulator radiation into N₂⁺($X^2\Sigma_g^+$, $v_X = 0$ or 1) which is then probed by LIF excitation spectroscopy in the laser wavelength of the ($B^2\Sigma_u^+$, $v_B = 0$ or 1) \leftarrow ($X^2\Sigma_g^+$, $v_X = 0$ or 1) transition, respectively. Partial cross sections for production of N₂⁺($X^2\Sigma_g^+$, $v_X = 0$ and 1) are measured as a function of the undulator photon energy. The cross section curves show peaks originating from transitions to Rydberg states converging to N₂⁺($A^2\Pi_u$, $v_A = 0-4$). Relative peak intensities differ from the $v_X = 0$ to 1 curves. Vibrational BR s resulting from autoionization of N₂⁺($A^2\Pi_u$) were studied by a Franck-Condon Analysis.

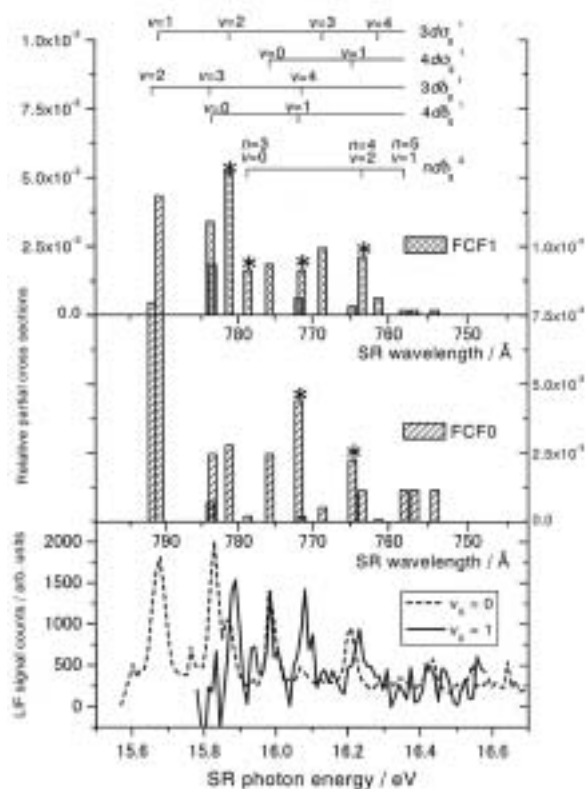


Figure 1. (Lowest Panel) Yield curves of N_2^+ ($X^2\Sigma_g^+$, $v_X = 0$ or 1) from N_2 obtained from the LIF count rate of the (B , $v_B = 0$ and 1) \rightarrow (X , $v_X = 1$ or 2) transitions, respectively. (Upper two panels) Partial cross sections for production of $N_2^+(X^2\Sigma_g^+$, $v_X = 0$ and 1) calculated by Franck-Condon Analysis.

VI-K Extreme UV Photoionization Studies by Employing a Dragon-Type Grazing-Incidence Monochromator

On the beam line BL2B2 in UVSOR a grazing incidence monochromator has been constructed which supplies photons in the energy region from 20 to 200 eV [M. Ono, H. Yoshida, H. Hattori and K. Mitsuke, *Nucl. Instrum. Methods Phys. Res., Sect. A* **467-468**, 577 (2001)]. This monochromator has bridged the energy gap between the beam lines BL3A2 and BL8B1, thus providing for an accelerating demand for the high-resolution and high-flux photon beam from the research fields of photoexcitation of inner-valence electrons, L -shell electrons in the third-row atom, and $4d$ electrons of the lanthanides.

Since 2001 we have tried taking photoion yield curves of fullerenes at BL2B2. Geometrical structures and electronic properties of fullerenes have attracted widespread attention because of their novel structures, novel reactivity, and novel catalytic behaviors as typical nanometer-size materials. Moreover, it has been emphasized that the potential for the development of fullerenes to superconductors ($T_c \sim 50$ K) and strong ferromagnetic substances is extremely high. In spite of such important species spectroscopic information is very limited in the extreme UV region, which has been probably due to difficulties in obtaining enough amount of sample. The situation has been rapidly changed in these few years, since the techniques of syntheses, isolation, and purification have been advanced so rapidly that appreciable amount of fullerenes is obtainable from several distributors in Japan.

VI-K-1 Anisotropy of Fragment Ions from SF_6 by Photoexcitation of a Valence- or Sulfur $2p$ -Electron between 23 and 210 eV

ONO, Masaki¹; MITSUKE, Koichiro
(¹Louisiana State Univ.)

[*Chem. Phys. Lett.* in press]

The anisotropy of the fragment ions produced by photoexcitation of SF_6 has been measured using synchrotron radiation in the energy range of 23–210 eV. In

spite of the highly symmetrical molecule the strong anisotropy is observed at lower photon energies. Anisotropy gradually decreases with increasing photon energy. The behavior of the curve of the asymmetry parameter has been interpreted qualitatively by means of simulation using partial oscillator strengths for the formation of fragment ions in the region of valence electron excitation (16–63 eV). Only SF_5^+ ions are assumed to have an anisotropic angular distribution, which can be explained in terms of transitions into neutral excited states of valence type. With increasing photon energy the branching ratio for the SF_5^+ ion

decreases, while the contribution of direct photoionization may increase. As a result the asymmetry parameter involving all the fragment ions declines steadily with the photon energy. Moreover, inner valence-electron excitation between 35 and 50 eV is found to open new decay channels which produce photoions isotropically. The asymmetry parameter remains constant at 0.01–0.02 below the sulfur $2p_{3/2,1/2}$ edges (< 180 eV), whether the photon energy is chosen at on- or off-resonance. Above the edges it decreases down to almost zero, in accord with the opening of the LVV Auger decay channels.

VI-K-2 Construction of the Photoionization Spectrometer for Fullerenes and Metallofullerenes

MITSUKE, Koichiro; ONO, Masaki¹; KOU, Junkei; MORI, Takanori; HARUYAMA, Yusuke²; KUBOZONO, Yoshihiro
(¹Louisiana State Univ.; ²Okayama Univ.)

Figure 1 shows the photograph of the apparatus designed to carry out extreme UV photoionization of fullerenes. A copper sample holder is mounted inside a radiation shield made of stainless steel. The vapor of the fullerene discharged from a small orifice is subjected to irradiation of the synchrotron radiation supplied from the Dragon-type monochromator. A drift tube was equipped between parallel plate electrodes placed above the oven unit and the housing of a microchannel plate electron multiplier detector. Insertion of the drift tube allows us to drastically reduce bothering background counts due to stray electrons and impurities and then realize a stable operation of the oven.

In the case of C_{60} the sample of 99.98% purity was purchased and further purified by eliminating organic solvent such as benzene or toluene through heating the sample one day in vacuum at 300 °C. In order to prepare the number density of fullerenes high enough at the interaction volume we increased the temperature of an oven up to 500 °C. The sublimation rate measured by using a quartz-oscillator thickness monitor was around 100 – 150 ng/s. We were able to find the optimum experimental conditions that keep a steady flow of the C_{60} vapor at the interaction volume.

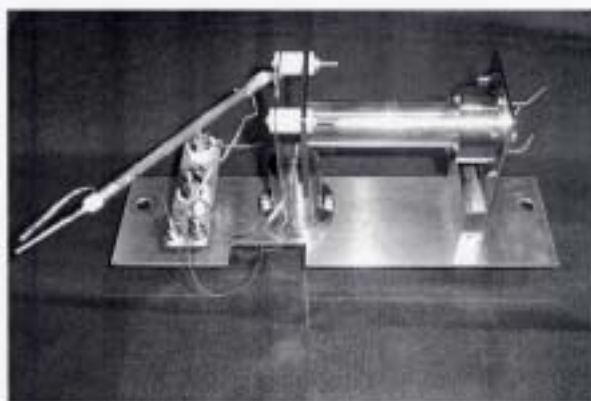


Figure 1. Photograph of the photoionization spectrometer developed for fullerenes.

VI-K-3 Photoion Yield Spectra of C_{60} in the Region of 23–210 eV

MITSUKE, Koichiro; ONO, Masaki¹; KOU, Junkei; MORI, Takanori; HARUYAMA, Yusuke²; KUBOZONO, Yoshihiro
(¹Louisiana State Univ.; ²Okayama Univ.)

In 1992 Hertel and coworkers have reported the photoionization efficiency curve for C_{60}^+ and revealed an intense broad peak at the photon energy of ~ 20 eV.¹⁾ They assigned it as resulting from excitation of surface plasmon in C_{60} : Collective longitudinal motion of multiple valence electrons is excited when C_{60} absorbs a transverse-wave light. So far much knowledge has been accumulated in the lower energy side of this plasmon peak, whereas there has been no experimental data between the high energy side and region containing the carbon $1s$ edge (~ 290 eV). This situation motivates us to take the efficiency curve encompassing the range from 23 to 210 eV.

Figure 1 shows a photoion yield curve of C_{60} plotted as a function of the photon energy. Above the three shoulders at 26, 33, and 47 eV the ion yield goes down monotonically with increasing photon energy. Figure 1 also shows representative data points from the literature.^{1,2)} Our data depend on the photon energy most weakly and behave similarly to those of Ref. 2) at ≤ 32 eV. The Hertel's spectrum completely differs from the other curves. The three shoulders, appearing only in our spectrum, are attributed to the shape resonance, *i.e.* promotion of an electron up to a vacant valence virtual orbital which is characterized by a high orbital angular momentum.

References

- 1) I.V. Hertel *et al.*, *Phys. Rev. Lett.* **68**, 784 (1992).
- 2) Yoo *et al.*, *J. Chem. Phys.* **96**, 911 (1992).

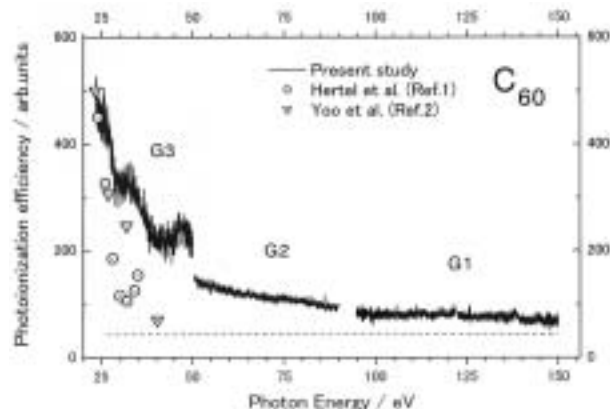


Figure 1. Photoionization efficiency curves of C_{60} .